

# Studies on the dissolution kinetics of ceramic uranium dioxide particles in nitric acid by microwave heating

Yunfeng Zhao, Jing Chen \*

*Institute of Nuclear and New Energy Technology, Tsinghua University, Beijing 102201, China*

Received 16 January 2007; accepted 27 March 2007

## Abstract

The kinetics of dissolution of uranium dioxide particles in 4–8 M ( $M = \text{mol/L}$ ) nitric acid by microwave heating has been studied. It is supposed that the  $\text{UO}_2$  particles dissolve homogeneously in the form of spherical particles. The dissolution process can be dealt with the well-known shrinking core model. The results show that under the 600 W microwave field, the dissolution of  $\text{UO}_2$  particles is controlled by the product layer diffusion at the temperature of 90–110 °C. The average activation energy for the dissolution of  $\text{UO}_2$  particles in 4–8 M nitric acid was calculated to be  $73.2 \pm 1.8 \text{ kJ/mol}$  from Arrhenius plots.

© 2007 Elsevier B.V. All rights reserved.

PACS: 81.05.Je; 82.30.Lp; 78.70.Gq

## 1. Introduction

Some studies on the dissolution of  $\text{UO}_2$  particles or powders have been reported. Taylor and his co-workers [1] studied the dissolution of sintered  $\text{UO}_2$  particles in  $\text{HNO}_3$  at various temperatures by the conventional heating. For unstirred dissolution rates below  $4 \text{ mg cm}^{-2} \text{ min}^{-1}$  at temperatures below 95 °C, the experimental activation energies are about  $15 \text{ kcal mol}^{-1}$  which lies in the range exhibited by catalyzed and heterogeneous chemical reactions; and at the higher dissolution rates near the boiling point, the activation energies fall to between 2 and  $5 \text{ kcal mol}^{-1}$  which may be compared with the value of  $4 \text{ kcal mol}^{-1}$  for the energy of diffusion. Ikeda et al. [2] studied the dissolution kinetics of the  $\text{UO}_2$  powders by conventional heating and found that the dissolution rate depended on the 2.3 power of  $[\text{NO}_3^-]_T$  in 4–8 M ( $M = \text{mol/L}$ )  $\text{HNO}_3$  solutions. The dissolution rate constant  $\phi$  in  $\text{mol cm}^{-2} \text{ min}^{-1}$  was expressed as  $\phi = (k_a + k_b[\text{HNO}_2])[\text{NO}_3^-]_T^{2.3}$ . The activation energies for  $k_a$  and  $k_b$  are  $79.5 \pm 6.7$  and  $36.8 \pm 2.9 \text{ kJ/mol}$ , respectively.

On the other hand, the applications of microwave energy in mineral processing were widely investigated after 1970. Microwave-assisted leaching has been studied to improve the yield of extracted metal and reduce the process time. The unique microwave heating advantages such as short processing time, direct, selective and volumetric heating, and a more controllable heating process [3] are the main driver for potential implementation in metal extraction.

In order to explore a new concept of head-end process for the treatment of spent fuel from high temperature gas-cooling reactor (HTGR), the dissolution of  $\text{UO}_2$  particles in the nitric acid solution by microwave heating is considered because the microwave energy can give a selective and rapid volumetric heating. In this paper, the dissolution of the  $\text{UO}_2$  particles in nitric acid media by the microwave heating has been studied fundamentally.

## 2. Experimental

### 2.1. Materials

The ceramic  $\text{UO}_2$  (depleted uranium) particles (450–550  $\mu\text{m}$ ) were made as the simulation kernel of the TRISO

\* Corresponding author.

E-mail addresses: [zhao-yf04@mails.tsinghua.edu.cn](mailto:zhao-yf04@mails.tsinghua.edu.cn) (Y. Zhao), [jingxia@tsinghua.edu.cn](mailto:jingxia@tsinghua.edu.cn) (J. Chen).

Table 1  
The character of the UO<sub>2</sub> particles

Molecular formula	Diameter (μm)	Density (g/cm <sup>-3</sup> )	O/U ratio
UO <sub>2</sub>	450–550	≥10.4	1.99–2.01
Method	Photo-electronic length measuring	Pycnometric density	Thermogravimetry (TG)

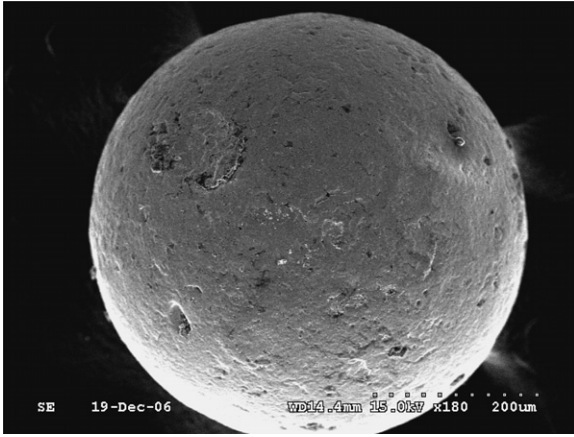


Fig. 1. Photos of the UO<sub>2</sub> particles.

coated fuel particles for fuel elements of the 10 MW high temperature gas-cooled reactor (HTR-10) in China. The characteristics of the particles are shown in Table 1. The diameter was determined by photo-electronic length measuring method [4]. Fig. 1 shows the photos of the UO<sub>2</sub> particles scanning by SEM. These UO<sub>2</sub> particles were made from the UO<sub>2</sub> (NO<sub>3</sub>)<sub>2</sub> solutions by the method called total-gelation process (TGU) [5], which includes the following steps: preparation, gelation, drying, deoxidizing, and sintered with hydrogen at 1500 °C. The products are called ‘ceramic’ UO<sub>2</sub> particles compared with the conventional UO<sub>2</sub> particles.

## 2.2. Apparatus

A MARS 5 (microwave assisted reactor system) with the Teflon vessels was used to study the dissolution of UO<sub>2</sub> particles under a 600 W, 2.45 GHz microwave field [6]. The temperature of solution in the vessel was automatically controlled by regulating the microwave power output according to a temperature feedback signal.

The concentrations of UO<sub>2</sub><sup>2+</sup> in the dissolution solution [7] were determined by the absorbance at 652 nm using spectrophotometer, with arsenazo III as the color-producing reagent [8].

## 2.3. Dissolution experiments

Firstly, 20 ml HNO<sub>3</sub> solution with an appropriate concentration was put in the Teflon vessel. UO<sub>2</sub> particles

(~0.0500 g) were weighed out accurately and charged into the Teflon vessel. Teflon vessel is transparent to microwaves so that the HNO<sub>3</sub> solutions can absorb the maximum amount of microwave energy.

The solution could be rapidly heated to a designated temperature in MARS 5 system. The temperature of the solution is detected by the fiber thermometer which does not absorb the microwave energy and with the accuracy of ±1 °C. The UO<sub>2</sub> was dissolved in the solution under the microwave field for a certain time, and then the solution was filtrated by the filter paper to separate the raffinate particles. The filtrated solution was analyzed by the spectrophotometer to determine the concentration of the uranium (VI).

## 3. Shrinking core model

The dissolution of UO<sub>2</sub> particles in the acidic media is a heterogeneous reaction, so the dissolution reaction kinetic model of UO<sub>2</sub> particles in HNO<sub>3</sub> can be associated with the well-known shrinking core models, which can be classified into the diffusion control through liquid film, the surface reaction control and the diffusion control through product layers [6,9]. In the case of spherical particles, these models can be expressed as follows:

$$x = k_F t \quad \text{for film diffusion control,} \quad (1)$$

$$1 - (1 - x)^{1/3} = k_S t \quad \text{for surface reaction control,} \quad (2)$$

$$1 + 2(1 - x) - 3(1 - x)^{2/3} = k_D t \quad \text{for product layer diffusion,} \quad (3)$$

where  $x$  is the reacted fraction at time  $t$  and  $k_F$ ,  $k_S$ ,  $k_D$  are apparent rate constants given in the following equations:

$$k_F = \frac{3bkC_{\text{HNO}_3}}{\rho}, \quad (4)$$

$$k_S = \frac{bkM(C_{\text{HNO}_3})^n}{\rho \cdot r_0}, \quad (5)$$

$$k_D = \frac{2bD_e M C_{\text{HNO}_3}}{\rho \cdot r_0^2}, \quad (6)$$

where  $b$ , stoichiometric coefficient;  $M$ , the molecular weight of reacted substance;  $\rho$ , the density of reacted particle;  $r_0$ , the initial particle radius;  $k$ , the intrinsic rate constant;  $D_e$ , effective diffusivity;  $C_{\text{HNO}_3}$ , the bulk concentration of HNO<sub>3</sub>;  $n$ , the reaction order in the term of HNO<sub>3</sub> concentration. Although these models are derived from the assumption that the particles are spherical, they are applicable for various-shaped particles [9].

## 4. Results and discussion

The experimental program was setup to study the dissolution kinetics of UO<sub>2</sub> particles in nitric acid at different temperatures. The results were analyzed with different kinetic models to explore the reaction mechanism.

4.1. Dissolution ratios at various temperatures in 4–8 M HNO<sub>3</sub>

The experiments were carried out in 4–8 M HNO<sub>3</sub> solution under a 600 W microwave field. The reaction temperatures were selected from 90 °C to 110 °C. The effect of temperature on the dissolution ratio of UO<sub>2</sub> particles are illustrated in Figs. 2–5. The experimental results show that the dissolution ratios increased quickly with the increase in temperatures. It was only 50% of the UO<sub>2</sub> particles dissolved in 4 M HNO<sub>3</sub> at 90 °C. However, when the temperature was increased to 110 °C, the dissolution ratio increased to 79%.

4.2. Effect of the HNO<sub>3</sub> concentration

The plots of the dissolution ratio *vs* time at different concentrations of HNO<sub>3</sub> are given in Figs. 6–9. It was found that the dissolution ratio increased with the reaction time and HNO<sub>3</sub> concentrations. At 100 °C within 40 min, only 59% of the UO<sub>2</sub> particles dissolved when the concentration of HNO<sub>3</sub> was 4 M; the value increased remarkably to 92% when the concentration of HNO<sub>3</sub> rose to 8 M.

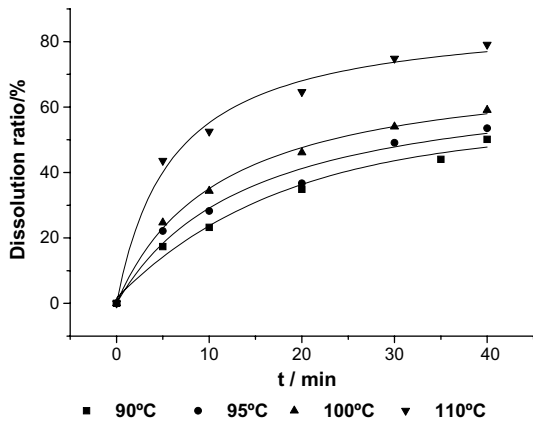


Fig. 2. Effect of temperatures on dissolution ratios in 4 M HNO<sub>3</sub>.

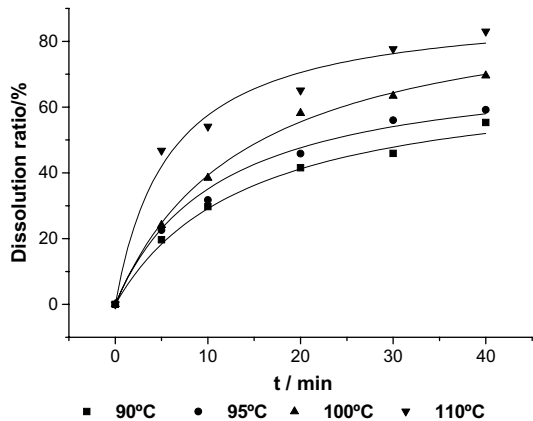


Fig. 3. Effect of temperatures on dissolution ratios in 5 M HNO<sub>3</sub>.

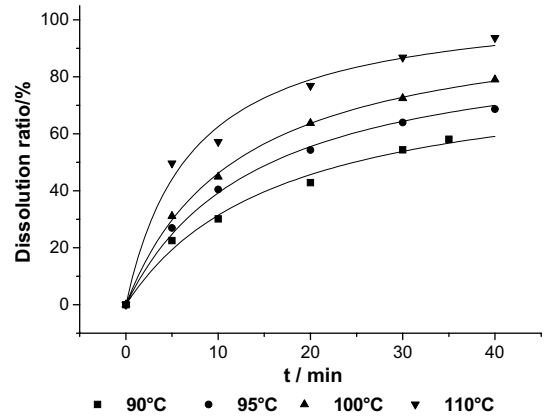


Fig. 4. Effect of temperature on dissolution ratios in 6 M HNO<sub>3</sub>.

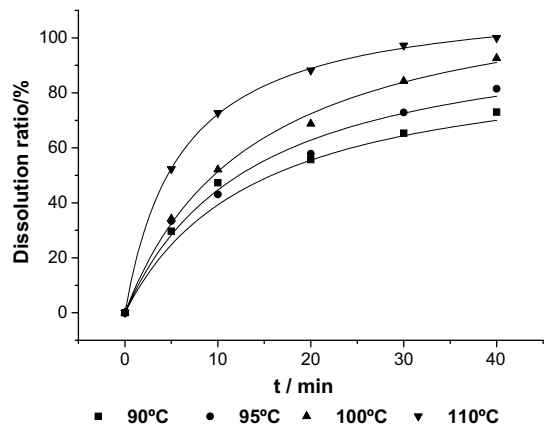


Fig. 5. Effect of temperature on dissolution ratios in 8 M HNO<sub>3</sub>.

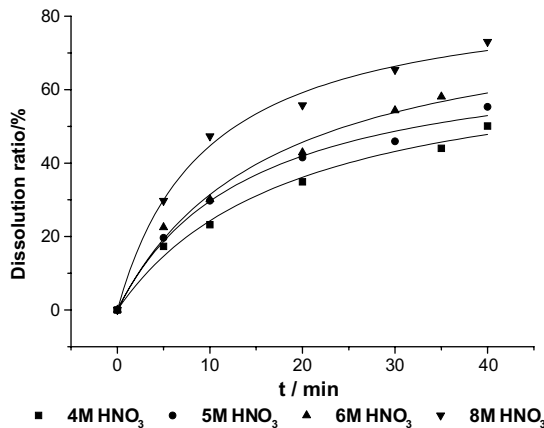


Fig. 6. Effect of HNO<sub>3</sub> concentrations on the dissolution at 90 °C.

4.3. Modeling of the dissolution kinetics

In the experiments, the dissolution process was under strong stirring, so the film diffusion was eliminated. The data in Figs. 2–5 were analyzed by the above shrinking core models (surface reaction control and product layer diffusion control); the results are given in Figs. 10–13 and

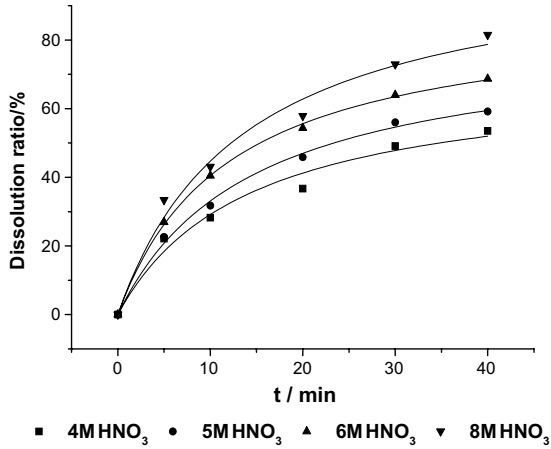


Fig. 7. Effect of HNO<sub>3</sub> concentrations on the dissolution at 95 °C.

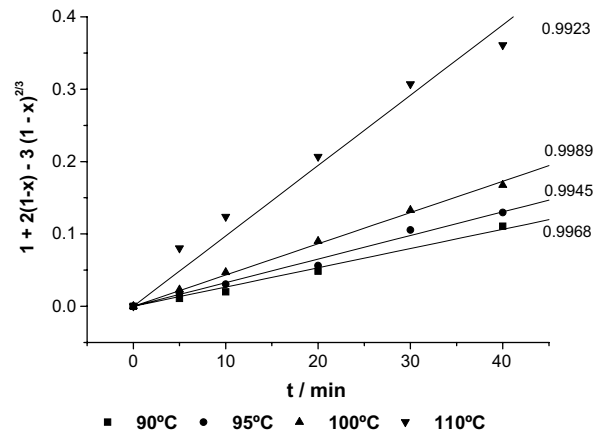


Fig. 10. Plot of  $1 + 2(1 - x) - 3(1 - x)^{2/3}$  vs reaction temperatures in 4 M HNO<sub>3</sub>.

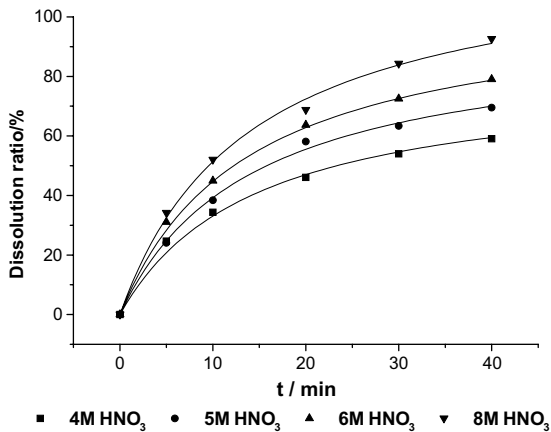


Fig. 8. Effect of HNO<sub>3</sub> concentrations on the dissolution at 100 °C.

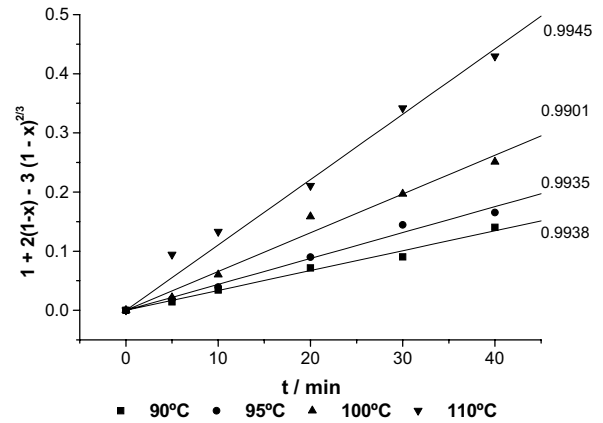


Fig. 11. Plot of  $1 + 2(1 - x) - 3(1 - x)^{2/3}$  vs reaction temperatures in 5 M HNO<sub>3</sub>.

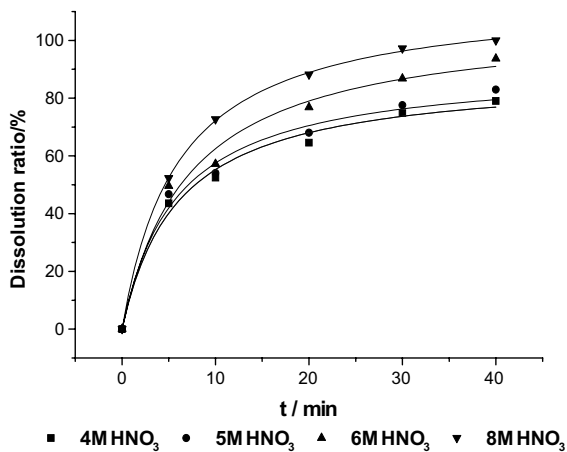


Fig. 9. Effect of HNO<sub>3</sub> concentrations on the dissolution at 110 °C.

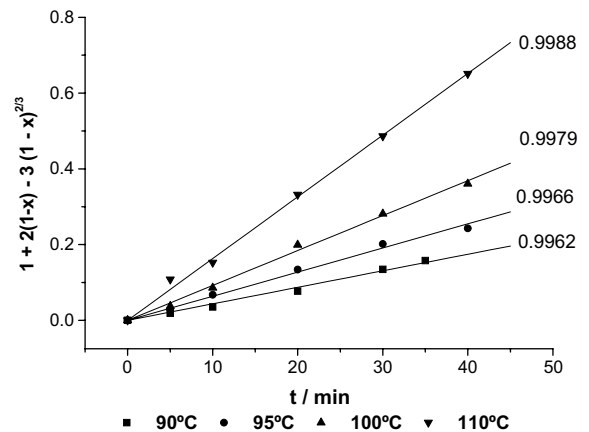


Fig. 12. Plot of  $1 + 2(1 - x) - 3(1 - x)^{2/3}$  vs reaction temperatures in 6 M HNO<sub>3</sub>.

Fig. 14 is an example of surface reaction control model for 8 M HNO<sub>3</sub>. From Figs. 13 and 14, it can be seen that the results fit very well with the product layer diffusion control model other than surface reaction control model because the correlation coefficients are above 0.99. The compari-

sons of the others are the same as Figs. 13 and 14, not illustrated here. The good linear relationships shown in Figs. 10–13 demonstrate that the application of Eq. (3) in the dissolution process is reliable. Within the reaction temper-

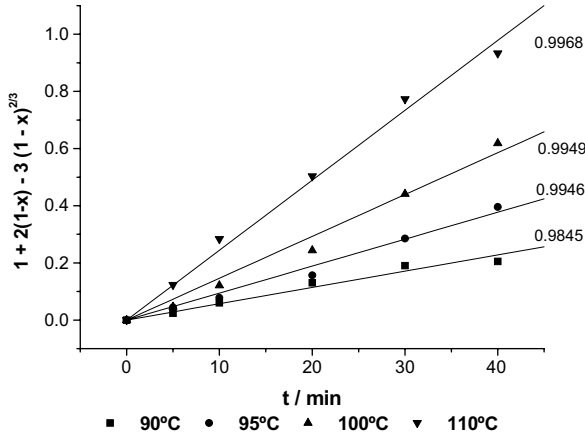


Fig. 13. Plot of  $1 + 2(1-x) - 3(1-x)^{2/3}$  vs reaction temperatures in 8 M  $\text{HNO}_3$ .

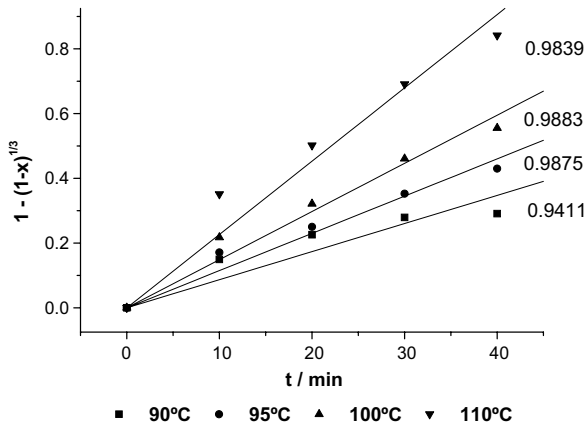


Fig. 14. Plot of  $1 - (1-x)^{1/3}$  vs reaction temperatures in 8 M  $\text{HNO}_3$ .

atures, the dissolution of  $\text{UO}_2$  particles are controlled by the product layer diffusion under the 600 W microwave field in 4–8 M  $\text{HNO}_3$  solutions.

According to Eq. (6), assuming that  $k_D = f(T, r_0, C_{\text{HNO}_3})$ , whereas  $r_0$  is initial particle radius in the experiment (450–550  $\mu\text{m}$ ),  $k_D$  can be expressed as follows:

$$k_D = k_0 e^{-\frac{E_a}{RT}} \cdot C_{\text{HNO}_3}^\alpha, \quad (7)$$

$$\text{Ln}(k_D) = \text{Ln}(k_0) - \frac{E_a}{RT} + \alpha \text{Ln}(C_{\text{HNO}_3}), \quad (8)$$

where  $k_0$  and  $\alpha$  are the constants to be determined.

The activation energy was calculated by the Arrhenius equation. The Arrhenius plots can be obtained from the values of reaction rate constant  $k_D$ , which can be obtained from the slopes of the plots at different temperatures and are shown in Fig. 15. The average activation energy for the dissolution of  $\text{UO}_2$  particles is  $73.2 \pm 1.8$  kJ/mol.

The plots of  $\text{Ln}(k_D)$  vs  $\text{Ln}(C_{\text{HNO}_3})$  are shown in Fig. 16. The slopes of these curves give the average  $\alpha$  value of  $1.58 \pm 0.05$ .

By using the stepwise linear regression method, the values of  $E_a$ ,  $k_0$  and  $\alpha$  can be obtained, respectively. The multi-

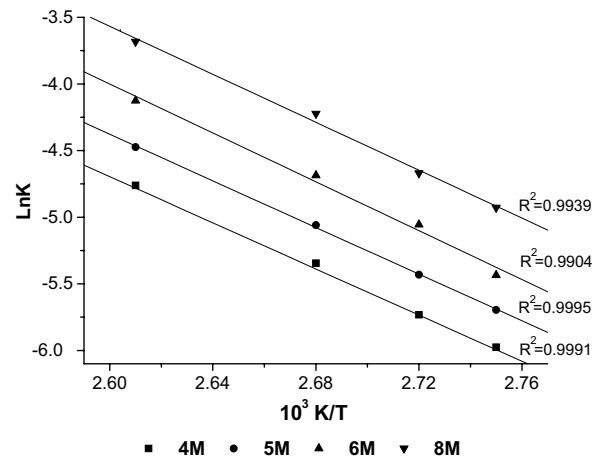


Fig. 15. Kinetic constants as a function of  $1/T$  in various  $\text{HNO}_3$  concentrations.

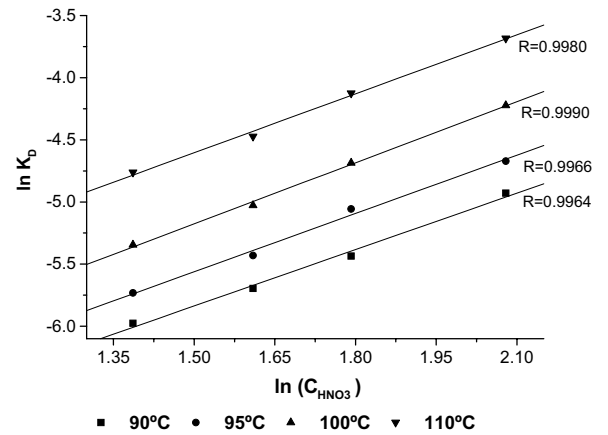


Fig. 16. The plots of  $\text{Ln}(k_D)$  vs  $\text{Ln}(C_{\text{HNO}_3})$ .

ple correlation coefficient is 0.998. Hence, the reaction rate constant can be expressed as

$$k_D = 9.10 \times 10^6 e^{-\frac{73200}{RT}} \cdot C_{\text{HNO}_3}^{1.58}. \quad (9)$$

Thus, according to Eq. (3), the dissolution of the ceramic  $\text{UO}_2$  particles under the present experimental conditions can be expressed as

$$1 + 2(1-x) - 3(1-x)^{2/3} = 9.10 \times 10^6 e^{-\frac{73200}{RT}} \cdot C_{\text{HNO}_3}^{1.58} \cdot t. \quad (10)$$

#### 4.4. Discussion

It can be seen from Eq. (10) that the dissolution ratios of the  $\text{UO}_2$  particles are dependent on the temperature and the  $\text{HNO}_3$  concentrations ( $\alpha = 1.58$ ). This fit very well with the fact that the dissolution ratios increased quickly with the increase in the reaction temperature and  $\text{HNO}_3$  concentration.

In comparison with the dissolution kinetics reported by Taylor et al. [1], the diffusion control covers wider

conditions by microwave heating. Taylor reported that the dissolution rate was controlled by the diffusion of reacting species when the temperature was lower than the boiling point (above 95 °C) and the concentration of the HNO<sub>3</sub> was more than 6 M. However, under the microwave field, the dissolution rate was controlled by the diffusion model at 90–110 °C with HNO<sub>3</sub> concentrations of 4–8 M. The activation energy by the microwave heating is about 73 kJ/mol, which is higher than what have been reported by Taylor. The reason may be that the different model used for analyzing the dissolution data, and the dissolution process was under strong stir in this paper, however, the solution was not stirred in the experiment reported by Taylor.

The difference of the dissolution rate between conventional heating and microwave heating probably results from the different experimental conditions. For conventional heating, the energy must be conducted through the walls of the vessel containing the solution. However, the microwave heating is different with the conventional heating. It can directly heat the uranium dioxide and the nitric acid solution [3], allowing the temperature to rise much faster. The nitric acid and the uranium dioxide are both polar molecules with high value of the dielectric loss factor and can absorb microwaves significantly [10,11]. The mixture of the reaction species are heated rapidly and the reaction rate is improved remarkably.

## 5. Conclusions

The dissolution rate of UO<sub>2</sub> particles is highly dependent on the temperature and the HNO<sub>3</sub> concentrations.

The dissolution rate increased with the reaction temperature and the HNO<sub>3</sub> concentrations. The studies on the dissolution kinetics show that the diffusion-controlled process can occur at lower temperature and HNO<sub>3</sub> concentration by microwave heating compared to conventional heating.

The dissolution of UO<sub>2</sub> in the HNO<sub>3</sub> solution under the microwave field of the experimental condition is controlled by the product layer diffusion control. The model constants can be determined by the linear regression of the reaction rate constant, and the dissolution kinetics of UO<sub>2</sub> particles at 90–110 °C can be expressed as Eq. (10).

## References

- [1] F. Taylor, W. Sharratt, L.E.M. De Chazal, D.H. Logsdail, *J. Appl. Chem.* 13 (1995) 32.
- [2] Y. Ikeda, Y. Yasuike, K. Nishimura, S. Hasegawa, Y. Takashima, *J. Nucl. Mater.* 224 (1995) 266.
- [3] M. Al-Harahsheh, S.W. Kingman, *Hydrometallurgy* 73 (2004) 189.
- [4] Bingzhong Zhang, Junguo Zhu, Bing Yang, Jintao Huang, *J. Tsinghua Univ. (Sci & Tech)* 36 (1996) 72.
- [5] Yaping Tang, Zhichang Xu, Fuhong Zhang, et al., *J. Tsinghua Univ. (Sci & Tech)* 37 (1997) 61.
- [6] J.H. Huang, N.A. Rowson, *Hydrometallurgy* 64 (2002) 169.
- [7] Y. Ikeda, Y. Yasuike, Y. Takashima, *J. Nucl. Sci. Technol.* 30 (1993) 962.
- [8] Yifei Guo, Junfu Liang, Rongzhou Jiao, Xiuqi Liu, *Atom. Energy Sci. Technol.* 34 (2000) 252.
- [9] O. Levenspiel, *Chemical Reaction Engineering*, Wiley, New York, 1972, p. 361.
- [10] P.A. Hass, *Am. Ceram. Soc. Bull.* 58 (1979) 873.
- [11] C.E. Holcombe, *Am. Ceram. Soc. Bull.* 62 (1983) 1388.